Stem Cell Research (2014) 12, 584–598

Available online at www.sciencedirect.com

ScienceDirect

www.elsevier.com/locate/scr

Combination of immortalization and inducible death strategies to generate a human mesenchymal stromal cell line with controlled survival☆

Paul Bourgine, Clementine Le Magnen, Sebastien Pigeot, Jeroen Geurts, Arnaud Scherberich, Ivan Martin*

Department of Biomedicine, Basel University Hospital, University of Basel, Basel, Switzerland

Received 22 November 2012; received in revised form 3 December 2013; accepted 17 December 2013
Available online 27 December 2013

Abstract The hTERT-immortalization of human bone marrow-derived Mesenchymal Stromal Cells (hMSCs) was proposed to address availability/standardization issues for experimental or clinical studies, but raised concerns due to possible uncontrolled growth or malignant cell transformation.

Here we report a method to generate a hMSCs line with controlled survival, through the implementation of a pre-established suicide system (inducible caspase 9, iCasp9) in hTERT-transduced hMSCs.

Primary hMSCs were successfully immortalized (>280 PD) and further transduced with the iCasp9 device. A clone was selected and shown to maintain typical properties of primary hMSCs, including phenotype, differentiation and immunomodulation capacities. The successive transductions did not induce tumorigenic transformation, as assessed by analysis of cell cycle regulators and *in vivo* luciferase-based cell tracking. Cells could be efficiently induced toward apoptosis (>95%) both *in vitro* and *in vivo*.

By combining the opposite concepts of 'induced-life' and 'inducible-death', we generated a hMSCs line with defined properties and allowing for temporally controlled survival. The cell line represents a relevant tool for medical discovery in regenerative medicine and a potential means to address availability, standardization and safety requirements in cell & gene therapy. The concept of a hTERT-iCasp9 combination, here explored in the context of hMSCs, could be extended to other types of progenitor/stem cells.

☆ Author contributions: Paul Bourgine: conception and design, collection and assembly of data, data analysis and interpretation, and manuscript writing; Clementine Le Magnen: collection and assembly of data; Sebastien Pigeot: collection and assembly of data; Jeroen Geurts: provision of study material, data analysis and interpretation; Arnaud Scherberich: conception and design, data analysis and interpretation; Ivan Martin: conception and design, financial support, manuscript writing, and final approval of manuscript.

* Corresponding author at: Tissue Engineering, Basel University Hospital, ICFS 405, Hebelstrasse 20, 4031 Basel, Switzerland. Fax: +41 61 265 3990.
E-mail address: imartin@uhbs.ch (I. Martin).

1873-5061/$ - see front matter © 2013 Published by Elsevier B.V.
http://dx.doi.org/10.1016/j.scr.2013.12.006

Introduction

Human bone marrow-derived Mesenchymal Stem/Stromal Cells (hMSCs) are widely investigated in regenerative medicine due to their multilineage differentiation capacity (Pittenger et al., 1999), immunomodulatory properties (Nauta and Fibbe, 2007), as well as their ability to migrate and deliver regulatory factors at injured sites or within tumor stroma (Kidd et al., 2009). Despite the large scientific interest and broad range of potential therapeutic applications, the coherent pre-clinical and clinical use of hMSCs is challenged by several critical issues, including the limited availability and the variability among different donors (Phinney et al., 1999).

The low amount of hMSCs in bone marrow aspirates (0.001 to 0.1% of nucleated cells) typically necessitates an *in vitro* expansion phase prior to use. The phase of amplification is limited by the replicative senescence phenomenon occurring under *in vitro* culture conditions, typically after 30 to 40 population doublings (PD) (Stenderup et al., 2003). Along with serial passages, the differentiation potential of hMSCs is reduced and functional changes have been reported (Minguell et al., 2001; Siddappa et al., 2007). The need for extensive hMSCs expansion, combined with their short life-span, is aggravated by the high variability among preparations from different donors, even if in the same age range (Siddappa et al., 2007).

To overcome hMSCs standardization and supply based problems, the generation of immortalized hMSCs was developed through the insertion of a human telomerase catalytic subunit (hTERT) (Boker et al., 2008;Huang et al., 2008;Jun et al., 2004;Piper et al., 2012;Simonsen et al., 2002a). The generation of hTERT-MSCs lines allowed extended hMSCs lifespan (>300 PD) and was shown to preserve some of the properties of primary hMSCs, such as their multilineage differentiation potential (toward osteogenesis, chondrogenesis and adipogenesis) (Abdallah et al., 2005; Jun et al., 2004; Mihara et al., 2003) and bone formation capacity (Simonsen et al., 2002b).

The enthusiasm raised by the availability of an unlimited cell source with stabilized properties was however tempered by safety aspects. A strong telomerase expression was in fact associated with many cancer types (Counter et al., 1998;Latil et al., 2000), and neoplastic changes have been reported following hTERT-transformation of hMSCs (Burns et al., 2005;Serakinci et al., 2004) resulting in uncontrolled cell growth. Such risk may be aggravated if hMSCs are delivered within a 3D matrix as opposed to systemic infusion, due to the previously reported enhanced long-term engraftment (Daga et al., 2002).

An elegant approach was recently proposed to enhance the safety of cellular therapies by the use of an inducible death-system (iDS) (Ramos et al., 2010;Straathof et al., 2005), based on the expression of a modified caspase 9 (iCasp9).

Beyond safety considerations, the introduction of an iDS may additionally offer the unprecedented opportunity to temporally control the survival of the transduced cells, in order to investigate their functional role in *in vitro* or *in vivo* models. However, while the device demonstrated a great efficiency in primary cells (Ramos et al., 2010; Straathof et al., 2005), no study has yet reported its functionality in immortalized cells. The concept may in fact be challenged by the fact that a hTERT over-expression has been previously associated to cell-suicide inhibition (Deeb et al., 2012; Indran et al., 2011; Liang et al., 2012), conferring notably a resistance to caspase-mediated apoptosis (Bermudez et al., 2006).

Toward the standardized, controlled and versatile use of hMSCs, we then aimed at assessing the feasibility to associate immortalization and 'inducible-death' concepts to generate a hTERT-hMSCs line efficiently inducible to apoptosis and maintaining the typical properties of primary hMSCs. The successful hTERT and iDS combination is expected to lead to the generation of an unlimited and well characterized hMSCs source with controlled survival, opening a variety of applications for research and pre-clinical purposes.

Materials and methods

Cell culture

Cell isolation

Human bone marrow aspirates were obtained during routine orthopedic surgical procedures involving exposure of the iliac crest, after ethical approval (EKBB, Ref.78/07) and informed donor consent. Marrow aspirates (20 ml volumes) were harvested from a healthy donor (female, 51 years old) using a bone marrow biopsy needle inserted through the cortical bone and immediately transferred into plastic tubes containing 15,000 IU heparin. After diluting the marrow aspirates with phosphate buffered saline (PBS) at a ratio of 1:4, nucleated cells were isolated using a density gradient solution (Histopaque, Sigma Chemical, Buchs, CH). Complete medium consisted of either Dulbecco's modified Eagle medium (DMEM) or α-minimum essential Medium (αMEM) with 10% fetal bovine serum, 1% HEPES (1 M), 1% Sodium pyruvate (100 mM) and 1% of Penicillin–Streptomycin–Glutamine (100×) solution (all from Gibco). Nucleated cells were plated at a density of 3.10^6 cells/cm^2 in complete medium supplemented with 5 ng/ml of fibroblast growth factor-2 (FGF-2, R&D Systems) and cultured in a humidified 37 °C/5% CO_2 incubator. In immortalized cell cultures, FGF-2 supply was interrupted after 140 PD, due to both the steady proliferation observed even in its absence and the possible impairment of the multi-lineage potential of hMSCs (Lai et al., 2011). Medium was changed twice in a week. hMSCs were selected on the basis of adhesion and proliferation on the plastic substrate 1 week after seeding.

Cell engineering

Immortalization

Immortalization was performed by the use of a lentivirus Lenti-hTERT-eGFP (LG508, Biogenova). Infection of hMSCs was performed 1 week after isolation and plating of the nucleated cell fraction from bone marrow aspirate. The virus was delivered at a Multiplicity Of Infection (MOI) of 5 in complete medium supplemented with 8 μg/mL of polybrene (Sigma Aldrich). The MOI was selected following preliminary experiments, in order to obtain high transduction efficiency while preserving the

cell functionality. The success of immortalization was assessed by flow cytometry (eGFP expression), telomerase activity measurement (TraP assay, Millipore, cat# S7700), a senescence assay (β-galactosidase assay, Sigma Aldrich, cat# CS0030) and by following the population doublings (PD) of the cells. The formula $PD_{(n/(n-1))} = (\log(N_n/N_{n-1}))/\log 2$ was used for the calculations of the PD at passage n, based on the number N of counted cells. The cumulative population doubling levels (PDL) are the sum of population doublings (PD) across each serial passage.

Retrovirus production

The retro-vector carrying the modified caspase 9 and CD19 (iCasp9-ΔCD19) was kindly provided by Dr. Carlos Almeida Ramos (Baylor College of Medicine, Houston, Texas, USA). The retrovirus was produced after transfecting the phoenix ECO cell line (American Type Culture Collection, cat# SD3444;) with the iCasp9-ΔCD19 vector. Virus containing supernatant was collected every 12 h, passed through a 0.45 μm filter and conserved at −80 °C.

The MSCV Luciferase PGK-hygro plasmid (Addgene plasmid 18782) was used for the production of retrovirus carrying the luciferase system (retro-Lucif). The virus production was performed using the same protocol as for the iCasp9-ΔCD19 retrovirus. Cells were selected by hygromycin B (Sigma, cat# H3274) treatment for 2 weeks.

Retroviral transduction

hMSCs were plated at 6000 cells/cm^2 in 60-mm dishes the day preceding the transduction. Cells were transduced by incubation with retroviral vector supernatants supplemented with 8 μg/μL of polybrene (Sigma Aldrich) for 5 min at 37 °C and centrifuged at 1100*g* for 30 min at room temperature in the dishes, followed by fresh medium replacement.

Cell Sorting

hMSCs stably expressing hTERT-eGFP and/or iCasp9-ΔCD19 were purified using a FACS-Vantage SE cell sorter (Becton Dickinson, Basel, Switzerland). Cells were sorted after immortalization and iCasp9-ΔCD19 transduction at 30 PDL and 195 PDL respectively. Prior to sorting of the CD19 positive fraction, cells were labeled using a human anti CD19-PerCP antibody (BD BIOSCIENCES, cat# 561295).

Cell characterization

Cell phenotyping

hMSCs phenotype was determined by cytofluometry analysis with fluorochrome-conjugated antibodies to human CD44 (cat# 559942), CD29 (cat# 555443), CD73 (cat# 560847), CD90 (cat# 559869), CD34 (cat# 555822), CD45 (cat# 555483), CD146 (cat# 550315), CD19 (cat# 561295), Epcam (cat# 347200) all from BD Pharmingen, and E-cadherin (cat#FAB18381P) from R&D Systems.

Adipogenic differentiation

hMSCs were differentiated as previously described (Barbero et al., 2003; Jaiswal et al., 1997; Jakob et al., 2001). Briefly, cells were seeded at 3000 cells/cm^2 and cultured for 1 week in DMEM complete medium without passage. During the following 2 weeks, cells were exposed to four differentiation cycles consisting in alternating 'strong' adipogenic medium (Dexamethasone 10^{-6} M, Indomethacin, Insulin, IBMX) for 3 days and 'light' adipogenic medium (Insulin) for 1 day.

Osteogenic differentiation

hMSCs were seeded at 3000 cells/cm^2 and differentiated for 3 weeks in osteogenic medium (OM). Osteogenic medium consists in αMEM complete medium supplemented with 10 nM Dexamethasone, 0.1 mM L-ascorbic acid-2-phosphate and 10 mM β-glycerophosphate (Maniatopoulos et al., 1988).

Chondrogenic differentiation

Culture of hMSCs was performed in 0.5 ml of DMEM containing 4.5 mg/ml D-Glucose, 0.1 mM nonessential amino acids, 1 mM sodium pyruvate, 100 mM HEPES buffer, 100 U/ml penicillin, 100 mg/ml streptomycin, and 0.29 mg/ml L-glutamine supplemented with 0.1 mM ascorbic acid 2-phosphate, 10 ng/ml TGFb1 and 10^{-7} M dexamethasone (Chondrogenic medium) as previously described (Jakob et al., 2001). Cells (350,000) were centrifuged in 1.5 ml conical polypropylene tubes (Sarstedt, Numbrecht, Germany) to form spherical pellets. After 2 weeks

Figure 1 Generation of hTERT-iDS hMSCs line. A) Functional map of the lenti-hTERT-eGFP (Biogenova, LG508) vector use for the immortalization of primary hMSCs. The system consists in a human telomerase gene and a eGFP reporter gene, under the control of separated CMV promoters.B) Telomerase activity of primary hMSCs and the immortalized population (Trap assay). The immortalized cells (hTERT-MSCs) displayed a higher telomerase activity (>4-fold) than their primary counterpart. Despite extensive doublings, the telomerase activity of the immortalized population remained stable (respectively assessed at 50, 100 and 150 PD).C) Population doubling levels of primary (black stars) and immortalized hMSCs (white dots). After 35 doublings, the primary cells stopped to proliferate while the M-SOD cells by passed the senescence-associated crisis. After 170 PD, the inducible death system (iDS) was introduced in the immortalized population. The M-SOD population underwent more than 270 PD after more than one year of culture.D) β-galactosidase assay of primary hMSCs (35 PD) and hTERT-iDS (50 PD) population. The primary hMSCs were shown to degrade β-galactosidase (blue coloration) when reaching 35 PD, indicating an entry in a replicative senescence phase. The immortalized population bypassed the senescence-associated crisis and continued to proliferate.E) Functional map of the iCasp9-ΔCD19 retrovector. The device drives the expression of a modified caspase 9 (iCaspas9) that can be induced toward dimerization thus leading to the activation of the apoptotic pathway. A 2A-like sequence between the iCaspase9 and CD19 gene ensures the cleavage of the CD19 surface marker from the iCaspase9, after transduction of the mRNA.F) CD19 expression of the hTERT-iDS cell line. A homogenous population (>98%) could be sorted after CD19 labeling of the successfully transduced cells, resulting in the isolation of the hTERT-iDS population.G) Functional assessment of the inducible death system implemented in the hTERT-iDS population. Prior to apoptosis activation, the majority (>93.6%) of the population was shown to be negative for Annexin-V and PI stainings (left panel). After activation of the system by an overnight exposure to the Chemical Inducer Dimerization (right panel), more than 99% of the cells were killed (positivity for Annexin-V or PI).

of culture, pellets were processed for histology and gene expression analysis.

Real-time PCR

Total RNA was extracted from cells using TRIzol (Invitrogen, Carlsbad, CA), treated with DNAse and retrotranscribed into DNA, as previously described (Frank et al., 2002). Real-time PCR was performed with the ABIPrism 77000 Sequence Detection System (Perkin Elmer/Applied Biosystem, Rotkreuz, Switzerland) and expression levels of genes of interest were normalized to GAPDH. Primers and probe sets of chondrogenic and osteogenic genes were used as previously described (Frank et al., 2002). Human PPARγ (Hs00234592_m1) Retinoblastoma 1, p53 (Hs01034249), p21 (Hs00355782_m1) primers and probe

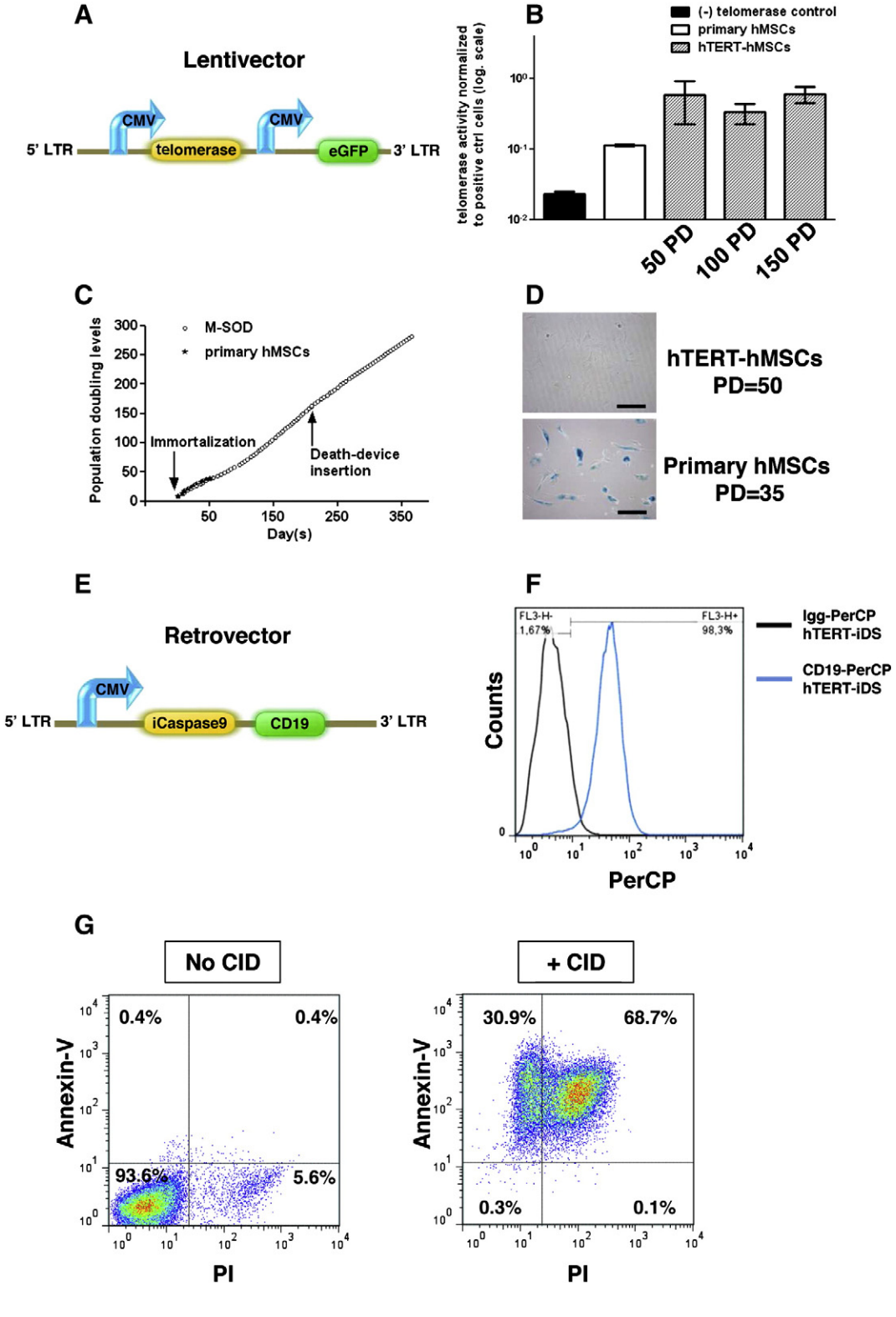

Table 1 Cytofluorimetric analysis of the primary cells and the generated cell line at different development time. The generated cell lines stably expressed conventional markers for hMSCs (CD44, CD29, CD73, CD90) while being negative for hematopoietic (CD34, CD45) and epithelial markers (Epcam, E-cadherin). The eGFP and CD19 expression respectively reflects the successful immortalization and iDS insertion. The successive genetic transformations and extensive doublings did not impair the mesenchymal phenotype of the cells.

	Primary hMSCs	hTERT—hMSCs			hTERT—iDS	
	PD=8	PD=75	PD=154	PD=170	Heterogenous PD=177	M—SOD PD>250
CD 44	+	+	+	+	+	+
CD 29	+	+	+	+	+	+
CD 73	+	+	+	+	+	+
CD 90	+	+	+	+	+	+
eGFP (hTERT)	—	+	+	+	+	+
CD 34	—	—	—	—	—	—
CD 45	—	—	—	—	—	—
CD 19 (death device)	—	—	—	—	+	+
CD 146	52.2%	N.a	67%	84%	+	+
Epcam	—	N.a	N.a	—	N.a	N.a
E—cadherin	—	N.a	N.a	—	N.a	N.a

\+ Positivity >90% — Negativity >90% N.a non assessed

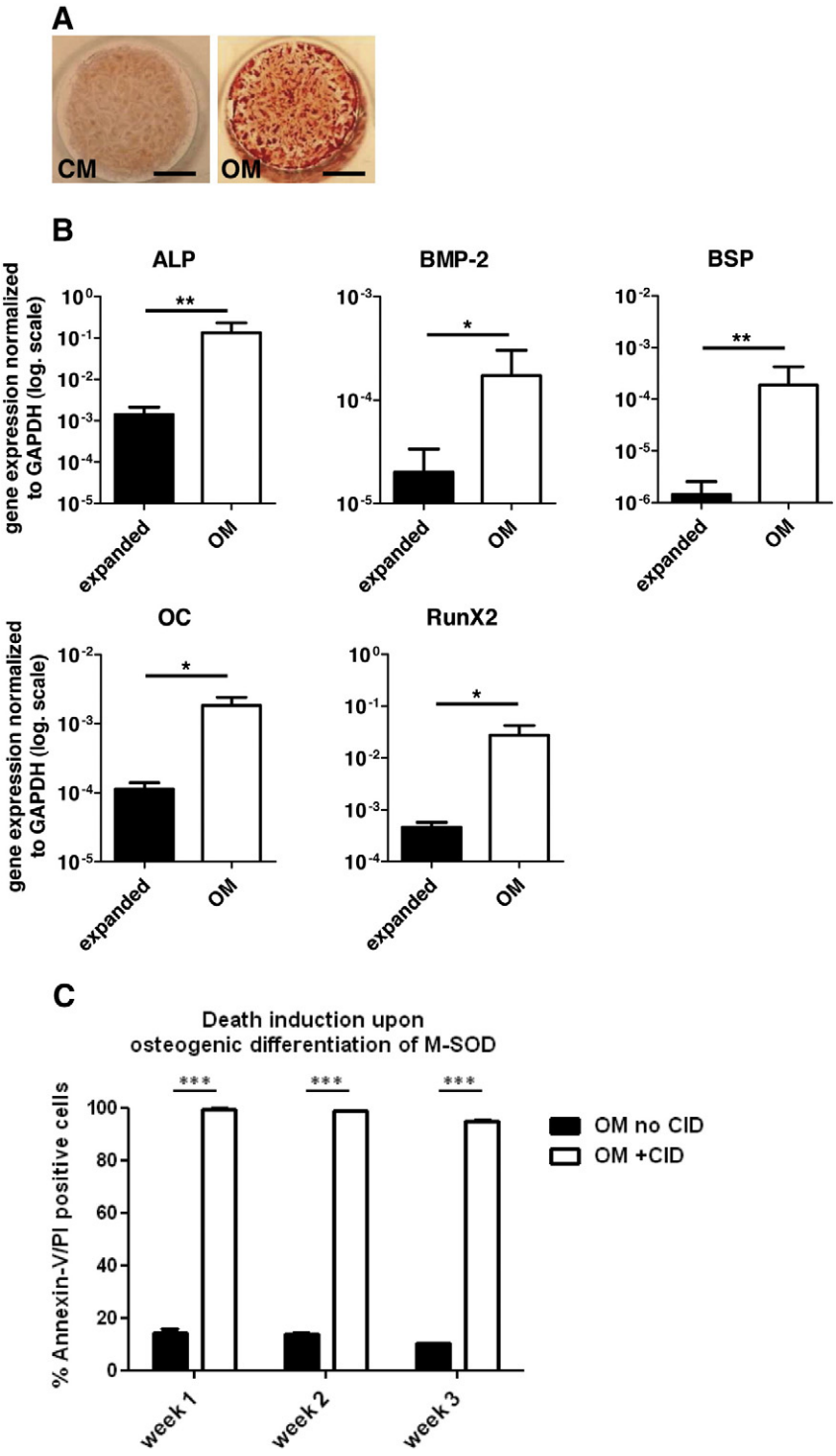

Figure 2 Osteogenic differentiation and killing assessment of M-SOD. A) Alizarin red staining of M-SOD cells after 3 weeks of culture in complete (CM) or osteogenic medium (OM). Only in presence of osteogenic medium, cells were able to deposit a mineralized matrix (red nodules). Size bar = 1 cm. B) Gene expression levels of key osteoblastic genes after 14 days of culture in osteogenic medium. As compared to cells assessed prior to culture in OM (expanded cells), a significant upregulation of Alkaline Phosphatase (ALP), Bone Morphogenetic Protein 2 (BMP-2), Bone Sialoprotein, Osteocalcin (OC) and RunX2 (Run-related transcription factor 2) was observed. *, $p < 0.05$. C) Induction of death during osteogenic differentiation of the SOD cell line. Cells were induced toward death (+CID) after 1, 2, or 3 weeks of culture in osteogenic medium (OM). Following exposure to CID, more than 95% of the cells became Annexin-V or PI positive, independently of their differentiation state. ***, $p < 0.001$.

were provided by Applied Biosystem. Probe and primers for c-Myc were ordered from Mycrosynth© and designed as follow:

forward GCCACGTCTCCACACATCAG
reverse TCTTGGCAGCAGGATAGTCCTT
probe ACGCAGCGCCTCCCTCCACTC

Biochemical stainings

Alizarin red, oil red-O and Alcian blue biochemical stainings were used to respectively assess the osteogenic, adipogenic and chondrogenic differentiation of the cells, as previously described (Barbero et al., 2003;Jaiswal et al., 1997;Jakob et al., 2001).

Karyotypic analysis

The karyotype of the M-SOD line was investigated by G-banding analysis. Briefly, cells in metaphase were fixed using fresh stationary liquid (methanol:glacial acetic acid = 3:1), spread on slides, stained with Giemsa solution, and observed under an immersion objective. n = 4.

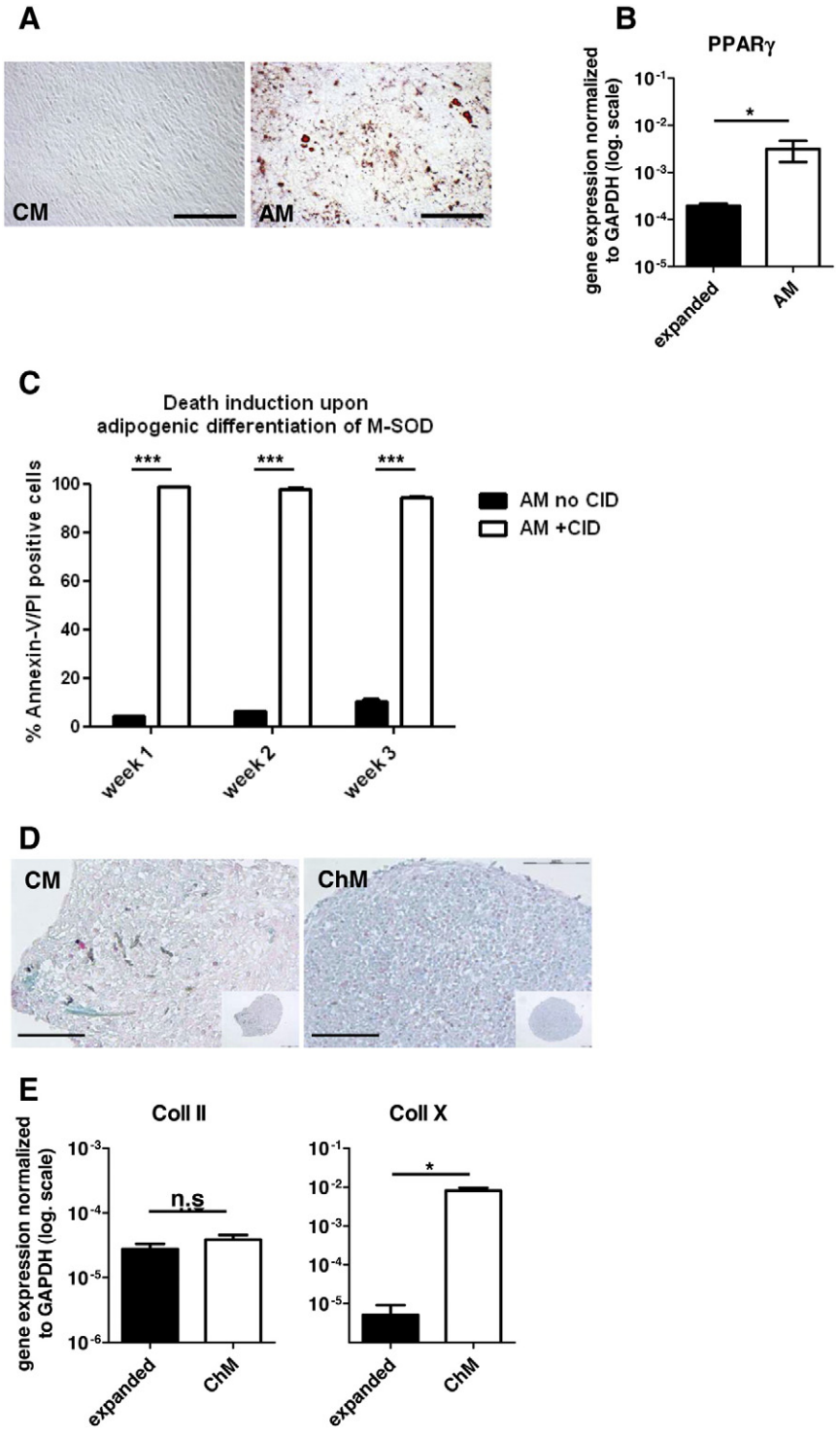

DNA profiling

The DNA profile of the primary hMSCs, the hTERT-hMSCs and of the M-SOD line was assessed by comparison of 15 DNA features inherited independently of each other, namely the following Short Tandem Repeats (STRs): D3S1358, THO1, D21S11, D18S51, Penta E, D5S818, D13S317, D7S820, D16S539, CSF1PO, Penta D, vWA, D8S1179, TPOX, FGA. The samples were analyzed by VIOLLIER AG (Basel, Switzerland).

Tumorigenicity assay

One million M-SOD cells previously transduced with the retro-Lucif virus were mixed with Matrigel Matrix (BD Biosciences) in a ratio 1:1 (V/V) with PBS and injected subcutaneously into the left flank of NOD/SCID mice (8–10 weeks old mice), initially obtained by Charles River Laboratories (Germany). Eventual tumor growth was monitored both weekly by palpation and by *in vivo* luminescence signal acquisition using an ISIS luminometer system. Prior to acquisition, mice received an intraperitoneal injection of 300 μL of D-Luciferin Potassium salt (Goldbiotechnology) at 15 mg/mL. Cells were tracked for a period of 6 months post-injection.

In vivo bone formation

In vivo ectopic bone formation was assessed as previously described (Braccini et al., 2005). Briefly, cells were resuspended in 30 μl of Fibrinogen (20 mg/ml Baxter, Austria), mixed with 30 μl of Thrombin (6 IU/ml Baxter, Austria) and immediately loaded onto 35 μg of bovine bone-derived granules (Actifuse, Apatech, Baxter, Austria). The constructs were transferred for 15 min in a humidified incubator at 37 °C with 5% CO2 to allow fibrin polymerization and implanted subcutaneously in CD-1 nu/nu nude mice (Charles River, Germany). After 8 weeks, the constructs were harvested, fixed overnight in 4% formalin, decalcified with a decalcification solution made of 7% EDTA (Sigma, cat# E5134) and 10% sucrose (Sigma, cat# S9378), paraffin embedded and 5 μm-thick-sections were obtained from different levels. Sections were stained with Masson's trichrome and observed microscopically to detect histological features of bone tissue. For fluorescence analysis, samples were fixed in 1.5% paraformaldehyde, decalcified with 7% EDTA (Sigma, cat# E5134), embedded in optimal cutting temperature, and snap frozen in liquid nitrogen. Sections (5 μm thick) were incubated with DAPI to stain nuclei. Fluorescence images were acquired using an Olympus BX-61 confocal microscope.

Immunomodulation assay (CFSE)

The immunomodulation of hMSCs was assessed as previously described (Gattinoni et al., 2011). Briefly, hMSCs were seeded in 96-well plates at 20.000, 10.000, 5000 and 2000 cells/well. $CD4^+$ lymphocytes were extracted from whole blood PBMCs by magnetic beads labeling (Miltenyi Biotec) and seeded on top of hMSCs at 1*10^5 cells per well after labeling with 2 μM CFSE (7 min at 37 °C). The $CD4^+$ cells were left untreated or stimulated with 1 μg/mL of phytohemagglutinin and the proliferation index was determined after 4 days by flow cytometry and analyzed with FlowJo software (Treestar).

Death induction

To induce cell death *in vitro*, the B/B homodimerizer (Clontech, cat# 635060) was added at 50 nM to iCasp9-ΔCD19 transduced hMSCs in culture medium to activate the apoptosis pathway through the dimerization of the modified caspase 9. Percentage of induced death was assessed 12 h later by FACS analysis, after cell harvest and staining with Annexin V-APC (BD Biosciences, cat#550475) and Propidium Iodide (PI, BD Biosciences, cat# 51-66211E) in Annexin-V binding buffer (BD Biosciences, cat# 556454). Control cells were cultured in the same medium without exposure to the homodimerizer.

The *in vivo* killing efficiency of the M-SOD line was assessed using 0.5 M cells previously transduced with the retro-Lucif virus, mixed with Matrigel Matrix (BD Biosciences) in a ratio 1:1 (V/V) with PBS and injected subcutaneously into the left flank of NOD/SCID mice (8–10 weeks old mice, Charles River Laboratories-Germany). To induce cell-death, mice (group 2, +CID) received the following day an injection of 50 μg of B/B homodimerizer (Clontech, cat# 635058) previously diluted in Tween 2% (SIGMA-ALDRICH, cat# P1379) and Kollisolv® PEG E 400 (SIGMA-ALDRICH, cat# 06855) according to the manufacturer instructions. The control group (group 1, no CID) consisted in mice receiving injection of diluent (Tween 2% and Kollisolv® PEG E 400) without B/B homodimerizer. The success of apoptotic induction was assessed by *in vivo* luminescence signal acquisition using an ISIS luminometer system. Prior to acquisition, mice received an intraperitoneal injection of 300 μL of D-Luciferin Potassium salt (Goldbiotechnology) at 15 mg/mL. The luminescence signal emitted by cells was measured up to 4 days post-killing induction.

Statistical analysis

Data are presented as means ± standard error. The significance of differences was evaluated using analysis of

Figure 3 Adipogenic/chondrogenic differentiation and killing assessment of M-SOD.A) Oil red-O staining of M-SOD after 3 weeks of culture in complete (CM) or adipogenic medium (AM). In presence of adipogenic medium, the M-SOD cell line was successfully differentiated into adipocytes as demonstrated by the positive staining of lipid droplets. Size bar = 200 μm.B) PPARγ gene expression level after 3 weeks of culture in complete or adipogenic medium. In adipogenic conditions, a significant overexpression of PPARγ mRNA level was detected (16.2 fold), thus confirming the capacity of M-SOD to differentiate into adipocytes. *, $p < 0.05$.C) Induction of death during adipogenic differentiation of the M-SOD cell line. Cells were efficiently induced toward death (+CID) after 1, 2 or 3 weeks of differentiation (>95%) in adipogenic medium (AM). A high killing efficiency (>95%) was reached despite the differentiation of the cells. ***, $p < 0.001$.D) Alcian blue staining of M-SOD pellets after 2 weeks of culture in complete (CM) or chondrogenic medium (ChM). Both culture conditions did not lead to the generation of a rich cartilaginous matrix (blue staining). Size bar = 100 μm.E) Collagen type II (Coll II) and type X (Coll 10) gene expression levels of M-SOD cells before (*expanded*) or after 2 weeks of pellet culture in chondrogenic medium (ChM). In chondrogenic conditions, only a significant overexpression of Coll 10 mRNA level was observed. ns = non-significant. *, $p < 0.05$.

variance (ANOVA) followed by the Bonferroni test for every set of data on which multiple comparisons were performed. For single comparison, Mann–Whitney test was used. $p < 0.05$ was considered to indicate statistical significance.

Results

Immortalization of human bone marrow derived mesenchymal stromal cells

Primary hMSCs were transduced with a lentivirus carrying the human telomerase gene (Fig. 1A). The rate of transduction was assessed by flow cytometry through the enhanced GFP (eGFP) reporter gene. After transduction, 78% of the cell population expressed the transgene. The eGFP positive fraction was sorted to increase the purity of the transduced population (Supp. data 1). The functionality of the implemented human telomerase gene was assessed by telomeric repeat amplification protocol (TRAP), allowing for a sensitive measurement of the telomerase activity. The immortalized population (hTERT-hMSCs) stably displayed higher telomerase activity (4.4 ± 1.5 fold) than their primary counterpart (primary hMSCs), even after extensive proliferation (shown up to 150 doublings, Fig. 1B). Primary hMSCs did not proliferate for more than 35 PD, while the immortalized hMSCs underwent more than 270 PD (Fig. 1C). Primary cells became senescent after 35 PD as assessed by β-galactosidase staining, while the transduced population bypassed the senescence associated crisis (Fig. 1D). The clonogenicity of the immortalized population was about 8-fold higher than for primary hMSCs (9.3% vs 80.3%). A stable hTERT-hMSCs line with steady proliferation capacity was thus successfully generated.

Generation of a clonal hTERT-iDS hMSCs line

After 170 PD, the hTERT-hMSCs line was transduced with the retrovirus carrying an inducible death system (iDS), including CD19 as reporter gene (Fig. 1E). After one round of transduction, more than 50% of the cells expressed CD19. After sorting, more than 98% of the cells expressed the reporter gene (Fig. 1F), resulting in the isolation of a stable hMSCs line uniformly carrying the death-inducible system (hTERT-iDS). The functionality of the iDS was investigated by exposing the hTERT-iDS line to the Chemical Inducer of Dimerization (CID), leading to the activation of the suicide system. Following overnight exposure to CID (Fig. 1G and supplemental online video 1), more than 99% of the cells were pushed toward death (PI-positive or Annexin-V-positive). No toxicity was induced by exposing primary hMSCs or hTERT-hMSCs to CID. An immortalized and death-inducible hMSCs line was thus successfully generated, demonstrating the possibility to combine a hTERT overexpression with an efficient iDS-mediated killing.

The immortalization process, combined with the insertion of the iDS and the extensive number of PD, gave rise to a likely heterogeneous cell line. In order to obtain a more uniform population, thirty single colonies were picked and 24 of those could be successfully expanded. We then arbitrarily decided to select the clone with the most prominent osteogenic differentiation capacity, as this is considered the common, default differentiation pathway for hMSCs (Muraglia et al., 2000). Following culture for 3 weeks in osteogenic differentiation medium, the clone displaying the strongest intensity of alizarin red staining was selected (Supp. data 2). The immortalized hMSC clone carrying the iDS was then denominated as the Mesenchymal-Sword Of Damocles (M-SOD) cell line for further characterization.

Purity assessment and phenotypic analysis of primary hMSCs and the generated cell line(s)

The phenotype of the cell line was cytofluorimetrically assessed at different doublings and after each genetic modification (Table 1). All transformed cells expressed typical hMSCs markers (positivity for CD44, CD29, CD73, and CD90) while being negative for both the hematopoietic markers CD34 and CD45 and the epithelial markers EpCam and E-cadherin. The immortalized population was also shown to increasingly express the CD146 marker following FGF-2 removal from the supplemented medium (at 140 PD), consistently with a previous study (Sacchetti et al., 2007). The successive genetic modifications and extensive proliferation of the cell line were thus shown to not lead to an alteration of the mesenchymal phenotype, as assessed by conventional markers.

In addition, despite extensive *in vitro* culture time the DNA profile of the primary hMSCs, hTERT-hMSCs and M-SOD remains identical, as demonstrated by STRs analysis (Supp. data 3). This demonstrates the absence of potential contaminations by other cell sources. Moreover, a karyotypic analysis of the M-SOD line revealed that M-SOD cells displayed the same chromosomal pattern, thus demonstrating the homogeneity of the generated cell line (data not shown).

Differentiation capacity of M-SOD line

The multilineage differentiation capacity of the M-SOD line was tested after different numbers of population doublings (ranging from 250 PD to over 280PD) in order to investigate the stability of M-SOD properties. Data presented below are the average of 4 different experimental runs.

After 3 weeks of culture in osteogenic medium (OM), M-SOD cells deposited a thick mineralized matrix, as demonstrated by positive alizarin red staining (Fig. 2A). A strong induction of key osteogenic genes (Fig. 2B) was detected after 2 weeks of culture in osteogenic conditions (94.8-, 8.5-, 130.9-, 16.1- and 58.7-fold for ALP, BMP-2, BSP, OC and RunX2 genes respectively, $p < 0.05$). The M-SOD line was thereby shown to be capable to efficiently differentiate toward the osteogenic lineage.

After 3 weeks of culture in adipogenic medium, M-SOD cells were successfully differentiated into adipocytes, as revealed by the positive Oil red-O staining of the lipid droplets (Fig. 3A). The upregulation of the adipogenic PPARγ gene (16.2-fold, Fig. 3B, $p < 0.05$) confirmed the capacity of the M-SOD line to differentiate toward the adipogenic lineage.

The chondrogenic differentiation capacity of the M-SOD line was assessed by Alcian blue staining after pellet culture in complete or chondrogenic medium (Fig. 3D). M-SOD cells did not generate a GAG-rich cartilaginous matrix and did not significantly upregulate Sox-9 (data not shown) or type II Collagen, despite a marked increase in type X Collagen gene expression level (291-fold, Fig. 3E, $p < 0.05$). Nevertheless, the primary donor from whom the M-SOD line was derived was also

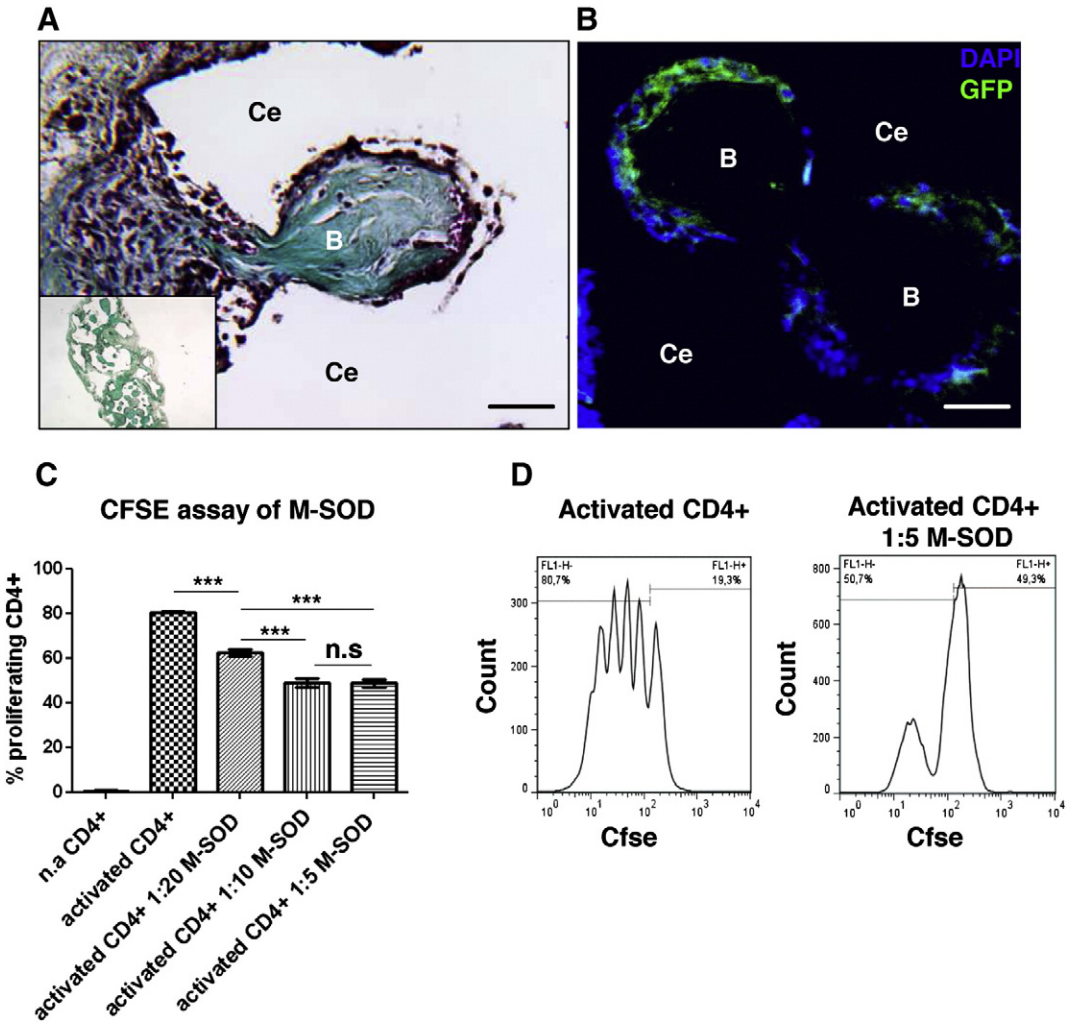

Figure 4 Bone formation and immunomodulatory capacities of M-SOD. A) *In vivo* bone formation of the M-SOD cell line. Cells successfully formed bone nodules (B) in contact with the ceramic granules (Ce), as demonstrated by Masson's trichrome staining (up) 8 weeks post *in vivo* implantation. Size bar = 50 μm and 1 mm for the lower magnification inset. B) Fluorescence microscopic analysis of bone formation of the M-SOD line. The eGFP signal (green) surrounding the bone nodules (B) demonstrates the contribution of M-SOD cells to the formed bone. Size bar = 50 μm. The blue signal refers to cell nuclei staining (DAPI). C) Immunomodulation assay (CFSE) of the M-SOD line. The percentage of proliferating $CD4^+$ after 4 days of culture, with different ratios of M-SOD cells, +/− PHA activation. D) Peaks of fluorescence in the activated $CD4^+$, alone or in co-culture (1:5) with M-SOD cells, 4 days post PHA activation. In the absence of M-SOD, 5 peaks of fluorescence were observed corresponding to 4 division cycles.

not capable to differentiate toward the chondrogenic lineage (Supp. data 4). This suggests that M-SOD low chondrogenic capacity may not be due to the successive genetic modifications or the extensive doublings.

Death induction upon osteogenic and adipogenic differentiation

The chromatin remodeling that occurs during cell differentiation (Benayahu et al., 2007;Siddiqi et al., 2010) can potentially lead to the silencing of the implemented iDS. Consequently, the functionality of the iDS system had to be demonstrated also during cell differentiation.

The death induction efficiency of the M-SOD line was tested during osteogenic or adipogenic differentiation, using cells expanded for different numbers of population doublings (ranging from 250 to over 280). Data presented below are the average of 3 different experimental runs.

During osteogenic differentiation, cells were induced with CID after 1, 2 or 3 weeks of culture in osteogenic medium. After an overnight exposure to CID, a very high killing efficiency was reached (97.7 ± 2.1%, Fig. 2C, $p < 0.0001$) irrespective of the cell differentiation stage. Similar results were obtained by inducing M-SOD cells during adipogenic differentiation (97.1 ± 2.5%, Fig. 3C, $p < 0.0001$). The iDS implemented within the M-SOD cell line thus remained highly efficient independently of the differentiation status.

Bone formation capacity of the M-SOD line

The bone formation capacity was assessed by combining 1 million of M-SOD cells together with ceramic granules, in a fibrinogen/thrombin gel, followed by ectopic implantation in

nude mice (n = 3) for 8 weeks. Samples were retrieved, fixed and decalcified prior to sectioning and histological analysis. The cells secreted a dense collagen matrix and the formation of bone nodules was observed within the constructs, as demonstrated by Masson's trichrome staining (Fig. 4A). GFP positive cells were observed at the outer regions of those nodules, indicating their contribution in the deposition of the osteoid tissue (Fig. 4B).

Immunomodulation capacity

hMSCs are known to exhibit immunomodulatory properties, which include the regulation of T-cell proliferation. This intrinsic hMSCs capacity has been proposed to be critical toward hMSCs application for graft *versus*-host or autoimmune diseases.

To assess whether the M-SOD line could regulate activated lymphocyte proliferation, $CD4^+$ cells were labeled

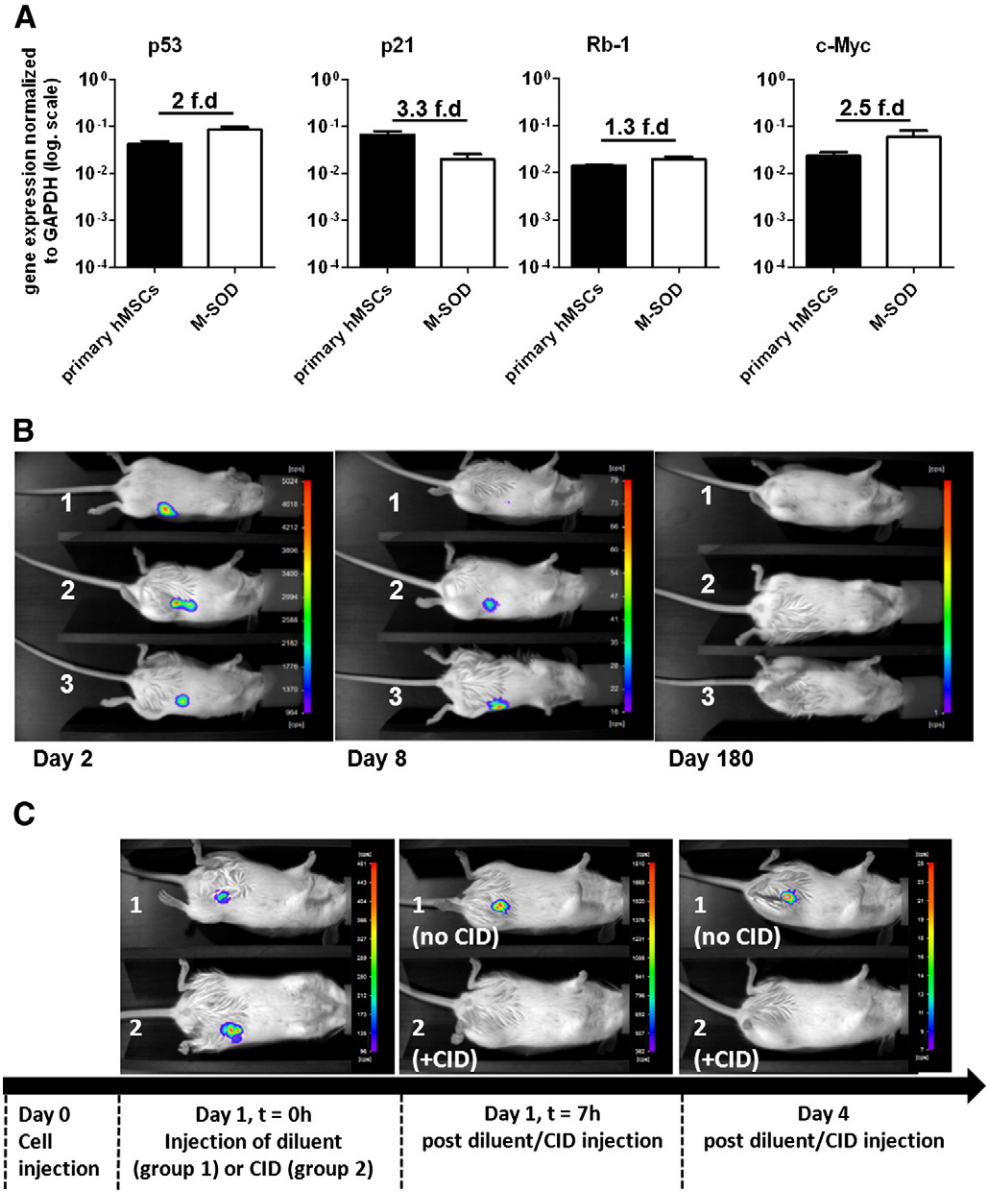

Figure 5 Assessment of M-SOD safety features. A) Gene expression levels of key oncogenes in expanded primary hMSCs and M-SOD. The primary hMSCs and M-SOD expressed similar levels of p53, p21, Rb1 and c-Myc. *, $p < 0.05$. f.d. = fold difference. B) Tumorigenicity assay of the M-SOD cell line. One million of M-SOD cells expressing luciferase were injected into the right flank of NOD/SCID mice (n = 3). Two days post cell injection, the luciferase system allows the localization of the M-SOD cells. After 8 days, the strength of the signal significantly decreased and was undetectable at day 16. More than 180 days post-injection, M-SOD cells remained undetectable so far demonstrating their non-tumorigenicity. C) *In vivo* killing efficiency of the M-SOD line. Half million of M-SOD cells expressing luciferase were injected into the right flank of NOD/SCID mice. One day post cell injection, mice were injected with 50 μg of CID (group 2, +CID) or only with the diluent (group 1, no CID). After 7 h, the luminescent signal disappeared only in mice having received the apoptotic inducer (+CID), thus demonstrating the possibility to specifically induce M-SOD apoptosis *in vivo*. The figures are representatives of n = 3 independent experimental runs using different mice.

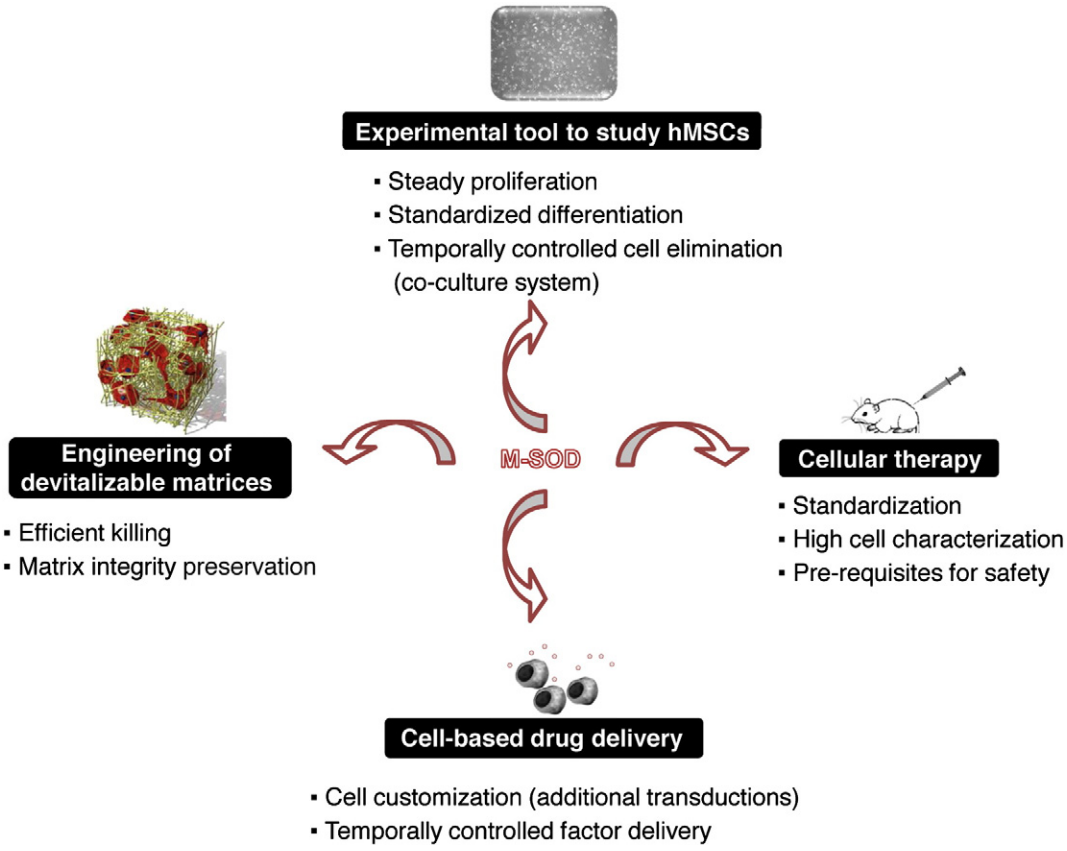

Figure 6 Schematic representations of the potential applications of the M-SOD line (see text for more extensive description).

with CFSE and co-cultured with M-SOD cells at different ratios. The proliferation of $CD4^+$ cells was measured 4 days post activation with phytohemagglutinin (PHA), by flow cytometry (Fig. 4C). In the absence of PHA, $CD4^+$ cells did not proliferate, independently of the presence or not of M-SOD cells, implying that M-SOD cells alone did not trigger an immune reaction. In the presence of PHA but in the absence of M-SOD, $CD4^+$ got activated and strongly proliferated (>80%), as shown by the 5 peaks of fluorescence observed, corresponding to 4 division cycles (Fig. 4D). M-SOD cells were able to inhibit such proliferation in a dose dependent manner (Fig. 4C). In particular, a 1:5 $CD4^+$/M-SOD ratio resulted in only one division of $CD4^+$ cells (Fig. 4D). The M-SOD cell line thus displayed antiproliferative properties on activated $CD4^+$ lymphocytes. In this regard, although further *in vivo* studies would be required to fully assess the regulatory properties, to the best of our knowledge the M-SOD line is the first reported bone-marrow derived hMSCs line capable of immunomodulation.

Oncogenes expression level. Tumorigenicity and *in vivo* killing assessment of M-SOD

Cell immortalization, as any genetic modification, can result in a malignant transformation by impairing the cell cycle regulation. Key proteins, such as p53, p21, retinoblastoma-1 or c-Myc, are known to play an important role as cell cycle regulators, keeping cell proliferation and DNA replication under control (Sharpless and Depinho, 2004). The genes p53, p21, retinoblastoma-1 (Rb-1) and c-Myc were expressed to a similar extent in M-SOD and the primary hMSCs (Fig. 5A), as shown by the limited fold differences (2.0 ± 0.4, 3.3 ± 3.1, 1.3 ± 0.2 and 2.5 ± 0.6 fold for p53, p21, Rb-1 and c-Myc respectively). The M-SOD cell line thus keeps expressing normal levels of cell cycle regulator genes.

The tumorigenicity of the M-SOD cell line was then investigated *in vivo* by subcutaneous injection in the flank of NOD/SCID mice of one million M-SOD cells, previously transduced with a luciferase reporter system (retro-Lucif). Within few days, the luminescence intensity remained focalized and rapidly decreased, suggesting the non-proliferation or dissemination of M-SOD cells (Fig. 5B). After more than 180 days post-injection, neither luminescence nor tumor formation was detected, indicating the non-tumorigenicity of M-SOD cells *in vivo*.

The iDS implemented into the M-SOD line also offers the possibility to control the survival of the cells *in vivo*. The *in vivo* killing efficiency was investigated by subcutaneously injecting the M-SOD cells previously transduced with a luciferase reporter system (retro-Lucif), in the flank of NOD/SCID mice. The implanted cells were induced toward apoptosis by intraperitoneal injection of CID. Seven hours post-killing induction, the M-SOD cells were shown to be successfully killed as reported by the loss of luminescent signal (Fig. 5C). Conversely, M-SOD cells transplanted in mice that did not receive a CID injection kept emitting a strong signal. The possibility to induce efficiently the killing of M-SOD cells *in vivo* was thus successfully demonstrated.

Discussion

By combining two typically opposing concepts, namely immortalization and death-induction, we generated a hMSCs line with standardized properties and temporal control over survival. In particular, the M-SOD line was shown to: a) steadily proliferate, b) differentiate toward the osteogenic and adipogenic lineages, c) maintain the *in vivo* bone forming capacity, d) regulate the proliferation of activated lymphocytes and e) be efficiently inducible toward death using a clinically approved compound (Ramos et al., 2010).

This study demonstrates the feasibility to induce an optimal killing of hMSCs despite their previous immortalization. The finding is not obvious, since the hTERT expression was previously shown to reduce the activation of caspases 3, 8, and 9, and of pro-apoptotic mitochondrial proteins, while increasing the expression of the anti-apoptotic mitochondrial protein Bcl-2 (Deeb et al., 2012; Indran et al., 2011; Liang et al., 2012). The constitutive expression of the inducible caspase 9 combined with its downstream role in the apoptotic pathway, allowed to bypass the hTERT-associated resistance to apoptosis (Deeb et al., 2012; Indran et al., 2011; Liang et al., 2012), ensuring a control over the cell survival in both un-differentiated and differentiated states.

The M-SOD properties appeared to derive from the primary cells. In fact, the strong osteogenic potency and limited chondrogenic potential could be related to the selection of the M-SOD clone as the one with the highest osteogenic differentiation capacity and to the poor chondrogenic ability of the primary hMSCs. Further studies are needed to confirm that the use of a primary donor or of a clone with a higher chondrogenic capacity would lead to the generation of a line capable to more efficiently undergo chondrogenesis.

The use of immortalized hMSCs with stabilized properties offers standardization opportunity for research purposes. This is in contrast to primary hMSCs, which after extensive *in vitro* culture undergo senescence or possibly degenerate into malignant cells (Ben-David et al., 2011;Stenderup et al., 2003; Tarte et al., 2010). The disposal of an unlimited cell source also allows a clonal screening and extensive characterization, as well as the long-term monitoring of the population. This might be particularly of interest when introducing further genetic modifications, allowing a full characterization from the integration site to the stability and expression level of the transgene.

Despite the random virus-derived integrations, known to potentially lead to malignant transformations (Du et al., 2005;Nienhuis et al., 2006), the M-SOD was demonstrated to be non-tumorigenic, both by assessment of the expression levels of cell proliferation and DNA replication gatekeepers, as well as by a standard *in vivo* test. The method can also be further optimized by combining hTERT and the iDS in a same lentivector, under the control of a unique promoter. Eventually, placing the hTERT gene behind the iDS at the 3′ end can ensure the systematic hTERT silencing in case of chromatin remodeling (through either a silencing in 5′ of the promoter or the direct silencing of hTERT in 3′). This principle would reduce the number of transductions and guarantee an intrinsic control of successfully immortalized cells by the iDS. Taken together, the non-tumorigenic engineering of M-SOD cells, combined with the control ensured by the iDS, supports the relevance of the developed strategy as a first step in the perspective of a clinical use. In this regard, safety concerns would anyway require to be more comprehensively addressed by a panel of additional methods (*e.g.* micro-array analysis), in order to propose the iDS-hTERT strategy for clinical purposes.

The diversity of hMSCs applications in regenerative medicine makes the M-SOD line an attractive experimental tool for a variety of contexts (Fig. 6). Beyond representing a standard and stable hMSCs source, the iDS activation could serve for the selective and temporally controlled cell elimination. This would be relevant in *in vitro* models, *e.g.* to study stage-specific cell–cell conditioning in co-culture systems, or in *in vivo* models, *e.g.* to address the question of how long the living hMSCs fraction is required in order to induce specific regenerative/tumor targeting effects or to be effective in the treatment of immune-related disorders. The M-SOD line can also be seen as a cellular platform that can undergo additional genetic modifications to overexpress defined factors and thus acting as drug carrier. This could be especially relevant to study the treatment of cancer, inflammatory or autoimmune diseases through the secretion of *e.g.* TRAIL or IFN-γ (Dai et al., 2011;Yang et al., 2009). In this regard, the demonstrated functionality of the iDS *in vivo* offers the possibility to switch off the expression of implemented transgenes and thus to temporally control the factor delivery. However, a stringent and quantitative assessment of the *in vivo* killing efficiency would require further transformation of the M-SOD line to express a gene allowing for their sensitive, non-invasive *in vivo* tracking (*e.g.*, production of species-mismatched erythropoietin (Daga et al., 2002)).

Finally, the M-SOD line represents a unique tool to engineer devitalized cell-laid matrices with the capacity to induce or regulate regenerative processes, *e.g.* to promote bone formation (Sadr et al., 2012). The M-SOD line would address standardization issues but also allow the devitalization of the engineered matrices upon iDS activation, prior to off-the-shelf storage. As compared to existing devitalization methods (*e.g.*, Freeze & thaw cycles or the use of detergents), the iDS would better preserve the matrix integrity while leading to an efficient killing of the cells in a streamlined manufacturing process.

Conclusions

The present study proposes and validates the concept of the first death-inducible cell line. Although the findings have been generated in the specific context of hMSCs, the paradigm can be extended to other cell types for distinct scientific and/or therapeutic applications. The work represents the basis toward the general perspective of using genetic tools not only to modify or understand cellular function, but also to standardize and increase the safety of cell-based therapies.

Supplementary data to this article can be found online at http://dx.doi.org/10.1016/j.scr.2013.12.006.

Disclosure of potential conflicts of interests

The authors declare no potential conflicts of interest.

List of abbreviations

ALP	Alkaline Phosphatase
AM	Adipogenic Medium
BMP-2	Bone Morphogenetic Protein 2
BSP	Bone SialoProtein
ChM	Chondrogenic Medium
CID	Chemical Inducer of Dimerization
CM	Complete Medium
CMV	CytoMegaloVirus
Coll II	Collagen type 2
Coll X	Collagen type 10
DAPI	4′,6-diamidino-2-phenylindole
Epcam	EPithelial Cell Adhesion Molecule
E-cadherin	Epithelial cadherin
FACS	Fluorescence-Activated Cell Sorting
FITC	Fluorescein IsoThioCyanate
GAG	GlycosAmynoGlycan
GAPDH	Glyceraldehyde 3-phosphate dehydrogenase
hMSCs	Human Mesenchymal Stromal Cells
hTERT	human TElomerase Reverse Transcriptase
iDS	inducible Death System
Igg	Immunoglobulin G
LTR	Long Terminal Repeat
MOI	Multiplicity Of Infection
M-SOD	Mesenchymal Sword Of Damocles
OC	Osteocalcin
OM	Osteogenic Medium
PD	Population Doubling
PerCP	PERidinin Chlorophyll Protein
PPARγ	Peroxisome proliferator activated receptor gamma
RunX2	Runt related transcription factor 2

Acknowledgments

We are grateful to Dr. Carlos A. Ramos (Center for Cell and Gene Therapy, Baylor College of Medicine, Houston, TX, USA) for kindly providing us with the iDS retrovector. We also thank Francesca Amicarella and Emanuele Trella (Oncology, Department of Biomedicine, Basel University Hospital, Basel, Switzerland) for their help regarding the immuno-modulation experiments. This work was supported by the European Community's Seventh Framework Program (MultiTERM, grant agreement number 238551). Financial support for JG was kindly provided by Dr. Andrea Banfi, Cell & Gene Therapy, Department of Biomedicine, University Hospital Basel, within the EU-FP7 project 'ANGIOSCAFF' (CP-IP 214402).

References

Abdallah, B.M., Haack-Sorensen, M., Burns, J.S., Elsnab, B., Jakob, F., Hokland, P., Kassem, M., 2005. Maintenance of differentiation potential of human bone marrow mesenchymal stem cells immortalized by human telomerase reverse transcriptase gene despite [corrected] extensive proliferation. Biochem. Biophys. Res. Commun. 326, 527–538.

Barbero, A., Ploegert, S., Heberer, M., Martin, I., 2003. Plasticity of clonal populations of dedifferentiated adult human articular chondrocytes. Arthritis Rheum. 48, 1315–1325.

Ben-David, U., Mayshar, Y., Benvenisty, N., 2011. Large-scale analysis reveals acquisition of lineage-specific chromosomal aberrations in human adult stem cells. Cell Stem Cell 9, 97–102.

Benayahu, D., Akavia, U.D., Shur, I., 2007. Differentiation of bone marrow stroma-derived mesenchymal cells. Curr. Med. Chem. 14, 173–179.

Bermudez, Y., Erasso, D., Johnson, N.C., Alfonso, M.Y., Lowell, N.E., Kruk, P.A., 2006. Telomerase confers resistance to caspase-mediated apoptosis. Clin. Interv. Aging 1, 155–167.

Boker, W., Yin, Z., Drosse, I., Haasters, F., Rossmann, O., Wierer, M., Popov, C., Locher, M., Mutschler, W., Docheva, D., Schieker, M., 2008. Introducing a single-cell-derived human mesenchymal stem cell line expressing hTERT after lentiviral gene transfer. J. Cell. Mol. Med. 12, 1347–1359.

Braccini, A., Wendt, D., Jaquiery, C., Jakob, M., Heberer, M., Kenins, L., Wodnar-Filipowicz, A., Quarto, R., Martin, I., 2005. Three-dimensional perfusion culture of human bone marrow cells and generation of osteoinductive grafts. Stem Cells 23, 1066–1072.

Burns, J.S., Abdallah, B.M., Guldberg, P., Rygaard, J., Schroder, H.D., Kassem, M., 2005. Tumorigenic heterogeneity in cancer stem cells evolved from long-term cultures of telomerase-immortalized human mesenchymal stem cells. Cancer Res. 65, 3126–3135.

Counter, C.M., Hahn, W.C., Wei, W., Caddle, S.D., Beijersbergen, R.L., Lansdorp, P.M., Sedivy, J.M., Weinberg, R.A., 1998. Dissociation among *in vitro* telomerase activity, telomere maintenance, and cellular immortalization. Proc. Natl. Acad. Sci. U. S. A. 95, 14723–14728.

Daga, A., Muraglia, A., Quarto, R., Cancedda, R., Corte, G., 2002. Enhanced engraftment of EPO-transduced human bone marrow stromal cells transplanted in a 3D matrix in non-conditioned NOD/SCID mice. Gene Ther. 9, 915–921.

Dai, L.J., Moniri, M.R., Zeng, Z.R., Zhou, J.X., Rayat, J., Warnock, G.L., 2011. Potential implications of mesenchymal stem cells in cancer therapy. Cancer Lett. 305, 8–20.

Deeb, D., Gao, X., Liu, Y., Kim, S.H., Pindolia, K.R., Arbab, A.S., Gautam, S.C., 2012. Inhibition of cell proliferation and induction of apoptosis by oleanane triterpenoid (CDDO-Me) in pancreatic cancer cells is associated with the suppression of hTERT gene expression and its telomerase activity. Biochem. Biophys. Res. Commun. 422, 561–567.

Du, Y., Jenkins, N.A., Copeland, N.G., 2005. Insertional mutagenesis identifies genes that promote the immortalization of primary bone marrow progenitor cells. Blood 106, 3932–3939.

Frank, O., Heim, M., Jakob, M., Barbero, A., Schafer, D., Bendik, I., Dick, W., Heberer, M., Martin, I., 2002. Real-time quantitative RT-PCR analysis of human bone marrow stromal cells during osteogenic differentiation *in vitro*. J. Cell. Biochem. 85, 737–746.

Gattinoni, L., Lugli, E., Ji, Y., Pos, Z., Paulos, C.M., Quigley, M.F., Almeida, J.R., Gostick, E., Yu, Z., Carpenito, C., Wang, E., Douek, D.C., Price, D.A., June, C.H., Marincola, F.M., Roederer, M., Restifo, N.P., 2011. A human memory T cell subset with stem cell-like properties. Nat. Med. 17, 1290–1297.

Huang, G., Zheng, Q., Sun, J., Guo, C., Yang, J., Chen, R., Xu, Y., Wang, G., Shen, D., Pan, Z., Jin, J., Wang, J., 2008. Stabilization of cellular properties and differentiation mutilpotential of human mesenchymal stem cells transduced with hTERT gene in a long-term culture. J. Cell. Biochem. 103, 1256–1269.

Indran, I.R., Hande, M.P., Pervaiz, S., 2011. hTERT overexpression alleviates intracellular ROS production, improves mitochondrial function, and inhibits ROS-mediated apoptosis in cancer cells. Cancer Res. 71, 266–276.

Jaiswal, N., Haynesworth, S.E., Caplan, A.I., Bruder, S.P., 1997. Osteogenic differentiation of purified, culture-expanded human mesenchymal stem cells *in vitro*. J. Cell. Biochem. 64, 295–312.

Jakob, M., Demarteau, O., Schafer, D., Hintermann, B., Dick, W., Heberer, M., Martin, I., 2001. Specific growth factors during the expansion and redifferentiation of adult human articular chondrocytes enhance chondrogenesis and cartilaginous tissue formation *in vitro*. J. Cell. Biochem. 81, 368–377.

Jun, E.S., Lee, T.H., Cho, H.H., Suh, S.Y., Jung, J.S., 2004. Expression of telomerase extends longevity and enhances differentiation in human adipose tissue-derived stromal cells. Cell. Physiol. Biochem. 14, 261–268.

Kidd, S., Spaeth, E., Dembinski, J.L., Dietrich, M., Watson, K., Klopp, A., Battula, V.L., Weil, M., Andreeff, M., Marini, F.C., 2009. Direct evidence of mesenchymal stem cell tropism for tumor and wounding microenvironments using *in vivo* bioluminescent imaging. Stem Cells 27, 2614–2623.

Lai, W.T., Krishnappa, V., Phinney, D.G., 2011. Fibroblast growth factor 2 (Fgf2) inhibits differentiation of mesenchymal stem cells by inducing Twist2 and Spry4, blocking extracellular regulated kinase activation, and altering Fgf receptor expression levels. Stem Cells 29, 1102–1111.

Latil, A., Vidaud, D., Valeri, A., Fournier, G., Vidaud, M., Lidereau, R., Cussenot, O., Biache, I., 2000. htert expression correlates with MYC over-expression in human prostate cancer. Int. J. Cancer 89, 172–176.

Liang, W., Ye, D., Dai, L., Shen, Y., Xu, J., 2012. Overexpression of hTERT extends replicative capacity of human nucleus pulposus cells, and protects against serum starvation-induced apoptosis and cell cycle arrest. J. Cell. Biochem. 113, 2112–2121.

Maniatopoulos, C., Sodek, J., Melcher, A.H., 1988. Bone formation *in vitro* by stromal cells obtained from bone marrow of young adult rats. Cell Tissue Res. 254, 317–330.

Mihara, K., Imai, C., Coustan-Smith, E., Dome, J.S., Dominici, M., Vanin, E., Campana, D., 2003. Development and functional characterization of human bone marrow mesenchymal cells immortalized by enforced expression of telomerase. Br. J. Haematol. 120, 846–849.

Minguell, J.J., Erices, A., Conget, P., 2001. Mesenchymal stem cells. Exp. Biol. Med. 226, 507–520 (Maywood).

Muraglia, A., Cancedda, R., Quarto, R., 2000. Clonal mesenchymal progenitors from human bone marrow differentiate *in vitro* according to a hierarchical model. J. Cell Sci. 113 (Pt 7), 1161–1166.

Nauta, A.J., Fibbe, W.E., 2007. Immunomodulatory properties of mesenchymal stromal cells. Blood 110, 3499–3506.

Nienhuis, A.W., Dunbar, C.E., Sorrentino, B.P., 2006. Genotoxicity of retroviral integration in hematopoietic cells. Mol. Ther. 13, 1031–1049.

Phinney, D.G., Kopen, G., Righter, W., Webster, S., Tremain, N., Prockop, D.J., 1999. Donor variation in the growth properties and osteogenic potential of human marrow stromal cells. J. Cell. Biochem. 75, 424–436.

Piper, S.L., Wang, M., Yamamoto, A., Malek, F., Luu, A., Kuo, A.C., Kim, H.T., 2012. Inducible immortality in hTERT-human mesenchymal stem cells. J. Orthop. Res. 30, 1879–1885.

Pittenger, M.F., Mackay, A.M., Beck, S.C., Jaiswal, R.K., Douglas, R., Mosca, J.D., Moorman, M.A., Simonetti, D.W., Craig, S., Marshak, D.R., 1999. Multilineage potential of adult human mesenchymal stem cells. Science 284, 143–147.

Ramos, C.A., Asgari, Z., Liu, E., Yvon, E., Heslop, H.E., Rooney, C.M., Brenner, M.K., Dotti, G., 2010. An inducible caspase 9 suicide gene to improve the safety of mesenchymal stromal cell therapies. Stem Cells 28, 1107–1115.

Sacchetti, B., Funari, A., Michienzi, S., Di, C.S., Piersanti, S., Saggio, I., Tagliafico, E., Ferrari, S., Robey, P.G., Riminucci, M., Bianco, P., 2007. Self-renewing osteoprogenitors in bone marrow sinusoids can organize a hematopoietic microenvironment. Cell 131, 324–336.

Sadr, N., Pippenger, B.E., Scherberich, A., Wendt, D., Mantero, S., Martin, I., Papadimitropoulos, A., 2012. Enhancing the biological performance of synthetic polymeric materials by decoration with engineered, decellularized extracellular matrix. Biomaterials 33, 5085–5093.

Serakinci, N., Guldberg, P., Burns, J.S., Abdallah, B., Schrodder, H., Jensen, T., Kassem, M., 2004. Adult human mesenchymal stem cell as a target for neoplastic transformation. Oncogene 23, 5095–5098.

Sharpless, N.E., Depinho, R.A., 2004. Telomeres, stem cells, senescence, and cancer. J. Clin. Invest. 113, 160–168.

Siddappa, R., Licht, R., van, B.C., de, B.J., 2007. Donor variation and loss of multipotency during *in vitro* expansion of human mesenchymal stem cells for bone tissue engineering. J. Orthop. Res. 25, 1029–1041.

Siddiqi, S., Mills, J., Matushansky, I., 2010. Epigenetic remodeling of chromatin architecture: exploring tumor differentiation therapies in mesenchymal stem cells and sarcomas. Curr. Stem. Cell. Res. Ther. 5, 63–73.

Simonsen, J.L., Rosada, C., Serakinci, N., Justesen, J., Stenderup, K., Rattan, S.I., Jensen, T.G., Kassem, M., 2002a. Telomerase expression extends the proliferative life-span and maintains the osteogenic potential of human bone marrow stromal cells. Nat. Biotechnol. 20, 592–596.

Simonsen, J.L., Rosada, C., Serakinci, N., Justesen, J., Stenderup, K., Rattan, S.I., Jensen, T.G., Kassem, M., 2002b. Telomerase expression extends the proliferative life-span and maintains the osteogenic potential of human bone marrow stromal cells. Nat. Biotechnol. 20, 592–596.

Stenderup, K., Justesen, J., Clausen, C., Kassem, M., 2003. Aging is associated with decreased maximal life span and accelerated senescence of bone marrow stromal cells. Bone 33, 919–926.

Straathof, K.C., Pule, M.A., Yotnda, P., Dotti, G., Vanin, E.F., Brenner, M.K., Heslop, H.E., Spencer, D.M., Rooney, C.M., 2005. An inducible caspase 9 safety switch for T-cell therapy. Blood 105, 4247–4254.

Tarte, K., Gaillard, J., Lataillade, J.J., Fouillard, L., Becker, M., Mossafa, H., Tchirkov, A., Rouard, H., Henry, C., Splingard, M., Dulong, J., Monnier, D., Gourmelon, P., Gorin, N.C., Sensebe, L., 2010. Clinical-grade production of human mesenchymal stromal cells: occurrence of aneuploidy without transformation. Blood 115, 1549–1553.

Yang, B., Wu, X., Mao, Y., Bao, W., Gao, L., Zhou, P., Xie, R., Zhou, L., Zhu, J., 2009. Dual-targeted antitumor effects against brainstem glioma by intravenous delivery of tumor necrosis factor-related, apoptosis-inducing, ligand-engineered human mesenchymal stem cells. Neurosurgery 65, 610–624.